

Space-time least-squares finite elements for parabolic equations *

Thomas Führer¹Michael Karkulik²¹Facultad de Matemáticas, Pontificia Universidad Católica de Chile, Santiago, Chile²Departamento de Matemática, Universidad Técnica Federico Santa María, Valparaíso, Chile**Abstract**

We present a space-time least squares finite element method for the heat equation. It is based on residual minimization in L^2 norms in space-time of an equivalent first order system. This implies that (i) the resulting bilinear form is symmetric and coercive and hence any conforming discretization is uniformly stable, (ii) stiffness matrices are symmetric, positive definite, and sparse, (iii) we have a local a-posteriori error estimator for free. In particular, our approach features full space-time adaptivity. We also present a-priori error analysis on simplicial space-time meshes which are highly structured. Numerical results conclude this work.

Key words: Parabolic PDEs, space-time finite element methods, stability.

AMS Subject Classification: 35K20, 65M12, 65M15, 65M60.

1 Introduction

By now, Galerkin finite element methods are ubiquitous for the numerical approximation of elliptic partial differential equations. For the numerical solution of initial-boundary value problems for parabolic partial differential equations

$$\begin{aligned}\partial_t u + \mathcal{L}u &= f \text{ in } (0, T) \times \Omega, \\ u &= 0 \text{ on } \partial\Omega, \\ u(0) &= u_0 \text{ on } \Omega,\end{aligned}$$

it is then quite natural to employ finite element methods only for the spatial part of the PDE, and discretize the resulting system of ODEs by a time stepping method such as implicit Euler. The derivation and error analysis of such semi-discretizations is by now standard textbook knowledge, cf. [25]. An advantage of time stepping schemes is that their oblivious nature allows for optimal storage requirements if one is only interested in the final state. As soon as one considers problems where the entire history of the evolution problem is of interest, such as control of PDE [9],

*Supported by Conicyt Chile through projects FONDECYT 1170672 and 11170050.

optimal control with PDE constraints [11], or data assimilation [5], this advantage becomes less beneficial. Furthermore, the flexibility of time stepping schemes with respect to space-time local mesh refinement is very limited, such that possible local space-time singularities prevent the optimal usage of computational resources. Moreover, following [8], quasi-optimality results such as a Céa’s lemma are not available for time-stepping schemes. As was pointed out in [24], this has two mayor implications. First, a-priori error bounds for time-stepping schemes are only of asymptotic nature and do not cover the entire computational range as for Galerkin finite element methods. Second, the established theory on convergence of adaptive finite element methods also relies heavily on quasi-optimality and does therefore not carry over to time stepping schemes. Finally, when it comes to the development of parallel solvers, the sequentiality of time stepping schemes imposes severe difficulties. For this and various other reasons, simultaneous space-time finite element discretizations, where time is treated as just another spatial variable, have been proposed in recent years. They all rely basically on the standard well-posed variational space-time formulation of parabolic equations, cf. [6, Ch. XVIII, § 3], see also [20, Ch. 5]. This variational formulation is of Petrov–Galerkin type. Uniform stability in the discretization parameter for pairs of discrete trial- and test-spaces is therefore an issue. This issue turns out to be non-trivial and might be identified as the main obstacle in obtaining a flexible space-time finite element method. There are various works considering this problem. Recently in [1, 2, 23], using minimal residual Petrov-Galerkin discretizations, uniform stability is obtained for discrete spaces with non-uniform but, still, global time steps. Another approach, taken in [21], already allows for general simplicial space-time meshes, but uniform stability was shown only with respect to a weaker, mesh-dependent norm. Unfortunately, uniform stability in the natural, mesh-independent energy norm in this setting is out of reach, cf. [23, Remark 3.5]. We also mention that this approach can be extended to mesh- and degree-dependent norms in an hp -context [7]. Then, in [22], in the case of homogeneous initial conditions, the authors obtain an coercive Galerkin formulation of the heat equation which involves the computation of a Hilbert type transform of test functions.

In the paper at hand, we reconsider the development of a space-time discretization for parabolic equations. For clarity of presentation we focus exclusively on the heat equation $\mathcal{L} = -\Delta$, although we have no reason to believe that our approach does not carry over to general elliptic spatial differential operators of second order. In order to effectively circumvent the problems we identified above, our method will be based on the minimization of the space-time least-squares functional

$$j(u, \boldsymbol{\sigma}) := \int_0^T \|\partial_t u - \operatorname{div} \boldsymbol{\sigma} - f\|_{L^2(\Omega)}^2 + \|\boldsymbol{\sigma} - \nabla u\|_{L^2(\Omega)}^2 dt + \|u(0) - u_0\|_{L^2(\Omega)}^2$$

over appropriately chosen spaces. We stress that this particular functional was already mentioned in [4, Ch. 9.1.4]. Moreover, we note that a time-stepping scheme based on a least-squares functional of the above type (but on local time slices) was developed in [15, 16].

Our motivation to consider space-time least-squares finite element schemes for solving parabolic problems are their attractive properties:

- *Uniform stability:* The numerical method is uniformly stable for *any* choice of conforming subspaces, i.e., the discrete inf–sup constant is independent of the approximation space. Particularly, this enables the use of arbitrary space-time meshes.
- *Built-in adaptivity:* The least-squares functional evaluated in a discrete solution is equivalent to the error between exact and discrete solution (in some norm). Since all norms in the functional are of L^2 type this allows to easily localize them into (space-time) element contributions which can be used to steer a standard adaptive algorithm.
- *Symmetric, positive definite, and sparse algebraic systems:* The bilinear form associated with the least-squares functional is symmetric and coercive, and therefore the stiffness matrix of the discretized problem is symmetric and positive definite. This enables the use of standard solvers, e.g., the preconditioned CG method. Moreover, we avoid the use of negative order Sobolev norms, so that by using locally supported basis functions the resulting stiffness matrix is sparse.

In Section 3 we introduce and analyze the space-time least-squares functional for a first-order reformulation of the heat equation. We show that the right space associated to the problem consists of pairs of functions $(u, \boldsymbol{\sigma})$ with component u in the standard energy space for parabolic problems and $\boldsymbol{\sigma}$ in L^2 , with the additional restriction that $\partial_t u - \operatorname{div} \boldsymbol{\sigma}$ in L^2 . The natural norm in this space is stronger than the standard energy norm for the heat equation. (This is similar to least-squares methods for elliptic problems, where one assumes that $\operatorname{div} \boldsymbol{\sigma}$ is in L^2 instead of a negative order Sobolev space.) Since one of our aims is also to provide an easy-to-implement numerical method, we consider in Section 4 one of the simplest approximation spaces, that is, piecewise affine and globally continuous functions (“low order finite element spaces”) for both variables on a space-time mesh. We present a-priori error analysis for simplicial space-time meshes which are uniform and highly structured. Convergence rates are shown provided that the solution is sufficiently regular. The final Section 5 deals with an extensive study of numerical examples for problems with spatial domains in one respectively two dimensions.

To close the introduction we like to mention the recent works [14, 18, 13, 17]. There is also plenty of literature on time stepping methods using least-squares FEMs. For an overview we refer to [4, Ch. 9]. In our recent work [10] we improved the existing literature on time stepping least-squares method and showed optimal a-priori error bounds without relying on the so-called splitting property.

2 Sobolev and Bochner spaces

For a bounded (spatial) Lipschitz domain $\Omega \subset \mathbb{R}^d$ we consider the standard Lebesgue and Sobolev spaces $L^2(\Omega)$ and $H^k(\Omega)$ for $k \geq 1$ with the standard norms. The space $H_0^1(\Omega)$ consists of all $H^1(\Omega)$ functions with vanishing trace on the boundary $\partial\Omega$. We define $H^{-1}(\Omega) := H_0^1(\Omega)'$ and $H_0^{-1}(\Omega) := H^1(\Omega)'$ as topological duals with respect to the extended $L^2(\Omega)$ scalar product $(\cdot, \cdot)_\Omega$. For a fixed, bounded time interval $J = (0, T)$ and a Banach space X we will use the space $L^2(X)$ of functions $f : J \rightarrow X$ which are strongly measurable with respect to the Lebesgue measure ds

on \mathbb{R} and

$$\|f\|_{L^2(X)}^2 := \int_J \|f(s)\|_X^2 ds < \infty.$$

A function $f \in L^2(X)$ is said to have a weak time-derivative $f' \in L^2(X)$, if

$$\int_J f'(s) \cdot \varphi(s) ds = - \int_J f(s) \cdot \varphi'(s) ds \quad \text{for all test functions } \varphi \in C_0^\infty(J).$$

We then define the Sobolev-Bochner space $H^k(X)$ of functions in $L^2(X)$ whose weak derivatives $f^{(\alpha)}$ of all orders $|\alpha| \leq k$ exist, endowed with the norm

$$\|f\|_{H^k(X)}^2 := \sum_{|\alpha| \leq k} \|f^{(\alpha)}\|_{L^2(X)}^2.$$

If we denote by $C(\bar{J}; X)$ the space of continuous functions $f : \bar{J} \rightarrow X$ endowed with the natural norm, then we have the following well-known result, cf. [26, Thm. 25.5].

Lemma 1. *Let $X \hookrightarrow H \hookrightarrow X'$ be a Gelfand triple. Then, the embedding*

$$L^2(X) \cap H^1(X') \hookrightarrow C(\bar{J}; H)$$

is continuous.

We will have to interchange spatial and temporal derivatives in Bochner spaces. To that end, we will employ the following lemma.

Lemma 2. *Let $L : X \rightarrow Y$ be a linear and bounded operator between two Banach spaces X and Y and $u \in H^1(X)$. Then it holds $Lu \in H^1(Y)$ and $(Lu)' = L(u')$.*

Proof. It is well known, cf. [27, V.5, Cor 2] that if $f : J \rightarrow X$ is Bochner integrable, then $Lf : J \rightarrow Y$ is Bochner integrable and

$$L \int_J f(t) dt = \int_J (Lf)(t) dt.$$

For $u \in H^1(X)$, we calculate for any $\varphi \in C_0^\infty(J)$

$$\int_J (Lu)(t) \varphi'(t) dt = L \int_J u(t) \varphi'(t) dt = -L \int_J u'(t) \varphi(t) dt = - \int_J L(u')(t) \varphi(t) dt.$$

□

3 Least-squares formulation of the heat equation

Let $\Omega \subset \mathbb{R}^d$ be a bounded (spatial) Lipschitz domain and $J = (0, T)$ a given finite time interval. For two functions $f \in L^2(L^2(\Omega))$, and $u_0 \in L^2(\Omega)$ we consider the problem to find $u \in L^2(H_0^1(\Omega)) \cap H^1(H^{-1}(\Omega))$ such that

$$\begin{aligned} \partial_t u - \Delta u &= f \text{ in } J \times \Omega, \\ u &= 0 \text{ on } J \times \partial\Omega, \\ u(0) &= u_0 \text{ on } \Omega. \end{aligned} \tag{1}$$

It is important to mention that problem (1) is well posed even if $f \in L^2(H^{-1}(\Omega))$, cf. [28, Thm. 23.A]:

Proposition 3. *Let $f \in L^2(H^{-1}(\Omega))$, $u_0 \in L^2(\Omega)$. Then, the solution of (1) enjoys the stability estimate*

$$\|u\|_{L^2(H_0^1(\Omega)) \cap H^1(H^{-1}(\Omega))} \lesssim \|f\|_{L^2(H^{-1}(\Omega))} + \|u_0\|_{L^2(\Omega)}.$$

However if $f \in L^2(L^2(\Omega))$, then there holds the additional regularity $u \in L^2(H_0^1(\Omega)) \cap H^1(L^2(\Omega))$. For $f \in L^2(L^2(\Omega))$, $u_0 \in L^2(\Omega)$ we define the least-squares functional

$$j(v, \boldsymbol{\psi}) := \|\boldsymbol{\psi} - \nabla v\|_{L^2(J \times \Omega)}^2 + \|\partial_t v - \operatorname{div} \boldsymbol{\psi} - f\|_{L^2(J \times \Omega)}^2 + \|v(0) - u_0\|_{L^2(\Omega)}^2. \tag{2}$$

The solution u of (1) satisfies $j(u, \nabla u) = 0$. The minimization of the functional j then gives rise to the bilinear form

$$b(u, \boldsymbol{\sigma}; v, \boldsymbol{\psi}) := (\nabla u - \boldsymbol{\sigma}, \nabla v - \boldsymbol{\psi})_{J \times \Omega} + (\partial_t u - \operatorname{div} \boldsymbol{\sigma}, \partial_t v - \operatorname{div} \boldsymbol{\psi})_{J \times \Omega} + (u(0), v(0))_{\Omega}.$$

and the linear functional

$$\ell(v, \boldsymbol{\psi}) := (f, \partial_t v - \operatorname{div} \boldsymbol{\psi})_{J \times \Omega} + (u_0, v(0))_{\Omega}.$$

Define the Hilbert space

$$U := \{(v, \boldsymbol{\psi}) \mid v \in L^2(H_0^1(\Omega)) \cap H^1(H^{-1}(\Omega)), \boldsymbol{\psi} \in L^2(J \times \Omega), \partial_t v - \operatorname{div} \boldsymbol{\psi} \in L^2(J \times \Omega)\}$$

with its natural norm

$$\|(v, \boldsymbol{\psi})\|_U^2 := \|v\|_{L^2(H_0^1(\Omega))}^2 + \|v\|_{H^1(H^{-1}(\Omega))}^2 + \|\boldsymbol{\psi}\|_{L^2(J \times \Omega)}^2 + \|\partial_t v - \operatorname{div} \boldsymbol{\psi}\|_{L^2(J \times \Omega)}^2.$$

Consider the problem to

$$\text{find } (u, \boldsymbol{\sigma}) \in U \text{ such that } b(u, \boldsymbol{\sigma}; v, \boldsymbol{\psi}) = \ell(v, \boldsymbol{\psi}) \quad \text{for all } (v, \boldsymbol{\psi}) \in U. \tag{3}$$

The solution u of (1) and $\boldsymbol{\sigma} := \nabla u$ solve (3). We can show the following.

Lemma 4. *The bilinear form b is bounded and coercive on U , and the linear functional ℓ is bounded on U .*

Proof. Boundedness of b and ℓ follows immediately by Cauchy-Schwarz and Lemma 1. To show coercivity of b , let $(v, \boldsymbol{\psi}) \in U$ be arbitrary. Then,

$$\partial_t v - \Delta v = \partial_t v - \operatorname{div} \boldsymbol{\psi} + \operatorname{div}(\boldsymbol{\psi} - \nabla v),$$

where the right-hand side is taken in $L^2(H^{-1}(\Omega))$. Due to the well-posedness of the parabolic problem (Proposition 3 with $f = \partial_t v - \operatorname{div} \boldsymbol{\psi} + \operatorname{div}(\boldsymbol{\psi} - \nabla v)$, $u_0 = v(0)$) and obvious bounds,

$$\begin{aligned} \|v\|_{L^2(H_0^1(\Omega)) \cap H^1(H^{-1}(\Omega))} &\lesssim \|\partial_t v - \operatorname{div} \boldsymbol{\psi}\|_{L^2(H^{-1}(\Omega))} \\ &\quad + \|\operatorname{div}(\boldsymbol{\psi} - \nabla v)\|_{L^2(H^{-1}(\Omega))} + \|v(0)\|_{L^2(\Omega)} \\ &\lesssim \|\partial_t v - \operatorname{div} \boldsymbol{\psi}\|_{L^2(J \times \Omega)} \\ &\quad + \|\boldsymbol{\psi} - \nabla v\|_{L^2(J \times \Omega)} + \|v(0)\|_{L^2(\Omega)}. \end{aligned}$$

The triangle inequality and the last bound also yields that

$$\begin{aligned} \|\boldsymbol{\psi}\|_{L^2(J \times \Omega)} &\leq \|\boldsymbol{\psi} - \nabla v\|_{L^2(J \times \Omega)} + \|\nabla v\|_{L^2(J \times \Omega)} \\ &\leq \|\boldsymbol{\psi} - \nabla v\|_{L^2(J \times \Omega)} + \|v\|_{L^2(H_0^1(\Omega))} \\ &\lesssim \|\partial_t v - \operatorname{div} \boldsymbol{\psi}\|_{L^2(J \times \Omega)} + \|\boldsymbol{\psi} - \nabla v\|_{L^2(J \times \Omega)} + \|v(0)\|_{L^2(\Omega)}. \end{aligned}$$

Hence

$$\begin{aligned} \|(u, \boldsymbol{\psi})\|_U^2 &= \|v\|_{L^2(H_0^1(\Omega)) \cap H^1(H^{-1}(\Omega))}^2 + \|\boldsymbol{\psi}\|_{L^2(J \times \Omega)}^2 + \|\partial_t v - \operatorname{div} \boldsymbol{\psi}\|_{L^2(J \times \Omega)}^2 \\ &\lesssim \|\partial_t v - \operatorname{div} \boldsymbol{\psi}\|_{L^2(J \times \Omega)}^2 + \|\boldsymbol{\psi} - \nabla v\|_{L^2(J \times \Omega)}^2 + \|v(0)\|_{L^2(\Omega)}^2 \\ &= b(v, \boldsymbol{\psi}; v, \boldsymbol{\psi}), \end{aligned}$$

which proves coercivity. \square

The last lemma immediately implies the first main result of this work.

Theorem 5. *Problem (3) is well-posed. Furthermore, if $U_h \subset U$ is a closed subspace, then the problem to*

$$\text{find } (u_h, \boldsymbol{\sigma}_h) \in U_h \text{ such that } b(u_h, \boldsymbol{\sigma}_h; v_h, \boldsymbol{\psi}_h) = \ell(v_h, \boldsymbol{\psi}_h) \quad \text{for all } (v_h, \boldsymbol{\psi}_h) \in U_h. \quad (4)$$

is well-posed and there holds the quasi-optimality

$$\|(u - u_h, \boldsymbol{\sigma} - \boldsymbol{\sigma}_h)\|_U \lesssim \min_{(w_h, \boldsymbol{\phi}_h) \in U_h} \|(u - w_h, \boldsymbol{\sigma} - \boldsymbol{\phi}_h)\|_U$$

Proof. Well-posedness follows immediately from Lemma 4 and the Lax–Milgram theorem. The quasi-optimality result is a standard consequence. \square

4 Numerical approximation by finite elements

Let \mathcal{T}_h be a simplicial and admissible partition of the space-time cylinder $J \times \Omega$. By admissible, we mean that there are no hanging nodes. Define

$$\begin{aligned}\mathcal{S}^1(\mathcal{T}_h) &= \{u \in C(J \times \Omega) \mid u|_K \text{ a polynomial of degree at most 1 for all } K \in \mathcal{T}_h\}, \\ \mathcal{S}_0^1(\mathcal{T}_h) &= \{u \in \mathcal{S}^1(\mathcal{T}_h) \mid u = 0 \text{ on } \bar{J} \times \partial\Omega\}.\end{aligned}$$

Note that $\mathcal{S}_0^1(\mathcal{T}_h)$ is a subspace of $L^2(J; H_0^1(\Omega)) \cap H^1(J; H^{-1}(\Omega))$, and $[\mathcal{S}^1(\mathcal{T}_h)]^d$ is a subspace of $L^2(J \times \Omega)^d$. Furthermore, if $v_h \in \mathcal{S}_0^1(\mathcal{T}_h)$ and $\psi_h \in [\mathcal{S}^1(\mathcal{T}_h)]^d$, then $\partial_t v_h - \operatorname{div} \psi_h \in L^2(J \times \Omega)$. Hence, we can define the discrete conforming subspace

$$U_h = \mathcal{S}_0^1(\mathcal{T}_h) \times [\mathcal{S}^1(\mathcal{T}_h)]^d \subset U.$$

A finite-element approximation of Problem (3) is then given by (4).

4.1 A-priori convergence theory

Due the quasi-optimality of Theorem 5, in order to provide a-priori error analysis it suffices to analyze the approximation properties of U_h . In the present section, we will show such approximation results, provided that the space-time mesh \mathcal{T}_h is uniform and structured. By structured, we mean that \mathcal{T}_h is obtained from a tensor-product mesh $J_h \otimes \Omega_h$ via refinement of the tensor-product space-time cylindrical elements into simplices, cf. Section 4.1.2. First, in Section 4.1.1, we will obtain auxiliary results for space-time interpolation on the tensor product mesh $J_h \otimes \Omega_h$. To that end, let $J_h = \{j_1, j_2, \dots\}$ with $j_k = (t_k, t_{k+1})$ be a partition of the time interval J into subintervals of length h , and let $\Omega_h = \{\omega_1, \omega_2, \dots\}$ be a partition of physical space $\Omega \subset \mathbb{R}^d$ into d -simplices of diameter h . Then, define the (discrete) spaces

$$\begin{aligned}\mathcal{S}^1(J_h; X) &:= \{u \in C(J; X) \mid u|_j \text{ is affine in time with values in } X \text{ for all } j \in J_h\}, \\ \mathcal{S}^1(\Omega_h) &:= \{u \in C(\Omega) \mid u|_\omega \text{ a polynomial of degree at most 1 for all } \omega \in \Omega_h\}, \\ \mathcal{S}_0^1(\Omega_h) &:= \{u \in \mathcal{S}^1(\Omega_h) \mid u = 0 \text{ on } \partial\Omega\}.\end{aligned}$$

4.1.1 Space-time interpolation on tensor product meshes

First we will show that a function u can be approximated in the norm of $L^2(H_0^1(\Omega)) \cap H^1(H^{-1}(\Omega))$ to first order by discrete functions in $\mathcal{S}^1(J_h; \mathcal{S}_0^1(\Omega_h))$, given that u possesses some additional regularity which is in accordance with regularity results for the heat equation. To that end, we consider first a discretization only in time, given by the piecewise linear interpolation operator

$$\mathcal{I}_h^\otimes u(t_k) := u(t_k).$$

Lemma 6. *Let $\mathcal{I}_h^\otimes : C(\bar{J}; L^2(\Omega)) \rightarrow \mathcal{S}^1(J_h; L^2(\Omega))$ be the piecewise linear interpolation operator. If $u \in H^1(X)$ for some Hilbert space X , it holds*

$$\|u - \mathcal{I}_h^\otimes u\|_{L^2(X)} \lesssim h \|u\|_{H^1(X)}.$$

If $u \in H^2(X)$ for some Hilbert space X , it holds

$$\|(u - \mathcal{I}_h^\otimes u)'\|_{L^2(X)} \lesssim h \|u\|_{H^2(X)}.$$

Proof. For $t \in (t_j, t_{j+1})$, we have according to [12, Prop. 2.5.9] for $u \in H^1(X)$

$$u(t) = u(t_j) + \int_{t_j}^t u'(s) ds = u(t_{j+1}) - \int_t^{t_{j+1}} u'(s) ds$$

in X . Hence,

$$\mathcal{I}_h^\otimes u(t) = \frac{u(t_{j+1})(t - t_j) + u(t_j)(t_{j+1} - t)}{h} = u(t) + \frac{(t - t_j) \int_t^{t_{j+1}} u'(s) ds - (t_{j+1} - t) \int_{t_j}^t u'(s) ds}{h},$$

and we conclude with Hölder that

$$\|u(t) - \mathcal{I}_h^\otimes u(t)\|_X^2 \lesssim h \int_{t_j}^{t_{j+1}} \|u'(s)\|_X^2 ds.$$

Another integration in t shows the first of the stipulated estimates. Likewise, for $t \in (t_j, t_{j+1})$ we can apply two times [12, Prop. 2.5.9] for $u \in H^2(X)$ to see

$$\begin{aligned} u(t_{j+1}) &= u(t) + (t_{j+1} - t)u'(t) + \int_t^{t_{j+1}} \int_t^s u''(r) dr ds, \\ u(t_j) &= u(t) + (t_j - t)u'(t) + \int_t^{t_j} \int_t^s u''(r) dr ds \end{aligned}$$

in X . Hence,

$$(u - \mathcal{I}_h^\otimes u)'(t) = u'(t) - \frac{u(t_{j+1}) - u(t_j)}{h} = \frac{1}{h} \int_t^{t_j} \int_t^s u''(r) dr ds - \frac{1}{h} \int_t^{t_{j+1}} \int_t^s u''(r) dr ds,$$

and we conclude with Hölder

$$\|(u - \mathcal{I}_h^\otimes u)'(t)\|_X^2 \lesssim h \int_{t_j}^{t_{j+1}} \|u''(r)\|_X^2 dr$$

Another integration in t shows the second of the stipulated estimates. □

Next, we consider fully discrete interpolation operators. In order to analyze their approximation properties, we will compare them to the semi-discrete operator \mathcal{I}_h^\otimes . We will employ the $L^2(\Omega)$ -orthogonal projections

$$\begin{aligned} \Pi_h &: L^2(\Omega) \rightarrow \mathcal{S}^1(\Omega_h), \\ \Pi_{0,h} &: L^2(\Omega) \rightarrow \mathcal{S}_0^1(\Omega_h). \end{aligned}$$

There holds the approximation property

$$\|\Pi_h u - u\|_{L^2(\Omega)} \lesssim h \|u\|_{H^1(\Omega)}. \quad (5)$$

Furthermore, it is well-known that Π_h is $H^1(\Omega)$ -stable uniformly in h on uniform meshes, i.e.,

$$\|\Pi_h u\|_{H^1(\Omega)} \lesssim \|u\|_{H^1(\Omega)}. \quad (6)$$

This, and the fact that Π_h is a projection, implies the approximation estimate

$$\|\Pi_h u - u\|_{H^1(\Omega)} \lesssim h \|u\|_{H^2(\Omega)}. \quad (7)$$

The statements (5)–(7) also hold if we replace Π_h by $\Pi_{0,h}$. Furthermore, it holds that

$$\|\Pi_{0,h} u - u\|_{L^2(\Omega)} \lesssim h^2 \|u\|_{H^2(\Omega)}, \quad (8)$$

$$\|\Pi_{0,h} u - u\|_{H^{-1}(\Omega)} \lesssim h^2 \|u\|_{H_0^1(\Omega)}, \quad (9)$$

where the second estimate follows from a duality argument.

Theorem 7. *Define the operator*

$$\mathcal{J}_h^\otimes : C(\bar{J}; L^2(\Omega)) \rightarrow \mathcal{S}^1(J_h; \mathcal{S}^1(\Omega_h))$$

by $\mathcal{J}_h^\otimes := \mathcal{I}_h^\otimes \circ (Id \otimes \Pi_h)$. Then it holds

$$\|u - \mathcal{J}_h^\otimes u\|_{L^2(L^2(\Omega))} \lesssim h(\|u\|_{H^1(L^2(\Omega))} + \|u\|_{L^\infty(H^1(\Omega))}),$$

$$\|u - \mathcal{J}_h^\otimes u\|_{L^2(H^1(\Omega))} \lesssim h(\|u\|_{H^1(H^1(\Omega))} + \|u\|_{L^\infty(H^2(\Omega))}).$$

Define the operator

$$\mathcal{J}_{0,h}^\otimes : C(\bar{J}; L^2(\Omega)) \rightarrow \mathcal{S}^1(J_h; \mathcal{S}_0^1(\Omega_h)),$$

by $\mathcal{J}_{0,h}^\otimes := \mathcal{I}_h^\otimes \circ (Id \otimes \Pi_{0,h})$. Then it holds

$$\|u - \mathcal{J}_{0,h}^\otimes u\|_{L^2(H_0^1(\Omega))} \lesssim h(\|u\|_{H^1(H_0^1(\Omega))} + \|u\|_{L^\infty(H^2(\Omega))}),$$

$$\|(u - \mathcal{J}_{0,h}^\otimes u)'\|_{L^2(H^{-1}(\Omega))} \lesssim h(\|u\|_{H^2(H^{-1}(\Omega))} + \|u\|_{L^\infty(H_0^1(\Omega))}),$$

$$\|(u - \mathcal{J}_{0,h}^\otimes u)'\|_{L^2(L^2(\Omega))} \lesssim h(\|u\|_{H^2(L^2(\Omega))} + \|u\|_{L^\infty(H^2(\Omega))}).$$

Proof. We will first prove the statement for the operator \mathcal{J}_h . Note that for $t \in (t_j, t_{j+1})$ it holds

$$\mathcal{J}_h^\otimes u(t) = \mathcal{I}_h^\otimes u(t) + \frac{[\Pi_h(u(t_{j+1})) - u(t_{j+1})](t - t_j) + [\Pi_h(u(t_j)) - u(t_j)](t_{j+1} - t)}{h}. \quad (10)$$

Using the approximation property (5) we conclude

$$\begin{aligned} \|u(t) - \mathcal{J}_h^\otimes u(t)\|_{L^2(\Omega)} &\leq \|u(t) - \mathcal{I}_h^\otimes u(t)\|_{L^2(\Omega)} + \sum_{k=0,1} \|\Pi_h(u(t_{j+k})) - u(t_{j+k})\|_{L^2(\Omega)} \\ &\leq \|u(t) - \mathcal{I}_h^\otimes u(t)\|_{L^2(\Omega)} + h \sum_{k=0,1} \|u(t_{j+k})\|_{H^1(\Omega)}. \end{aligned}$$

Another integration in t and application of Theorem 6 with $X = L^2(\Omega)$ shows the first of the stipulated estimates. Likewise, from (10) we conclude with the approximation property (7)

$$\|u(t) - \mathcal{J}_h^\otimes u(t)\|_{H^1(\Omega)} \leq \|u(t) - \mathcal{I}_h^\otimes u(t)\|_{H^1(\Omega)} + h \sum_{k=0,1} \|u(t_{j+k})\|_{H^2(\Omega)}.$$

Another integration in t and application of Theorem 6 with $X = H^1(\Omega)$ shows the second of the stipulated estimates. To prove the statements for the operator $\mathcal{J}_{0,h}^\otimes$ we note that the first estimate follows as in the case of \mathcal{J}_h^\otimes , only replacing Π_h by $\Pi_{0,h}$ and $H^1(\Omega)$ by $H_0^1(\Omega)$. Next,

$$(\mathcal{J}_{0,h}^\otimes u)'(t) = (\mathcal{I}_h^\otimes u)'(t) + \frac{[\Pi_{0,h}(u(t_{j+1})) - u(t_{j+1})] - [\Pi_{0,h}(u(t_j)) - u(t_j)]}{h}. \quad (11)$$

We conclude with (9) that

$$\begin{aligned} \|u'(t) - (\mathcal{J}_{0,h}^\otimes u)'(t)\|_{H^{-1}(\Omega)} &\leq \|u'(t) - (\mathcal{I}_h^\otimes u)'(t)\|_{H^{-1}(\Omega)} + \frac{1}{h} \sum_{k=0,1} \|\Pi_{0,h}(u(t_{j+k})) - u(t_{j+k})\|_{H^{-1}(\Omega)} \\ &\leq \|u'(t) - (\mathcal{I}_h^\otimes u)'(t)\|_{H^{-1}(\Omega)} + h \sum_{k=0,1} \|u(t_{j+k})\|_{H_0^1(\Omega)}. \end{aligned}$$

Another integration in t and application of Theorem 6 with $X = H^{-1}(\Omega)$ shows the second of the stipulated estimates for $\mathcal{J}_{0,h}^\otimes$. To show the third estimate we apply the same arguments, only this time using the approximation estimate (8). \square

4.1.2 Space-time interpolation on simplicial meshes

The tensor-product mesh $J_h \otimes \Omega_h$ consists of elements which are space-time cylinders with d -simplices from Ω_h as base. It is possible to construct from $J_h \otimes \Omega_h$ a simplicial, admissible mesh \mathcal{T}_h , following the recent work [19]. To that end, suppose that the vertices of Ω_h are numbered like p_1, p_2, \dots, p_N . An element $\omega \in \Omega_h$ can then be represented uniquely as the convex hull

$$\omega = \text{conv}(p_{i_1^\omega}, \dots, p_{i_{d+1}^\omega}), \text{ with } i_k^\omega < i_\ell^\omega \text{ for } k < \ell.$$

This ‘‘local numbering’’ of vertices is called *consistent numbering* in the literature, cf. [3]. An element $K = \omega \times j_k \in J_h \otimes \Omega_h$ can hence be written as convex hull

$$K = \text{conv}(p'_1, \dots, p'_{d+1}, p''_1, \dots, p''_{d+1}),$$

where

$$p'_\ell = (p_{i_\ell}, t_k), \quad p''_\ell = (p_{i_\ell}, t_{k+1}).$$

We can split K into $(d+1)$ different $d+1$ -simplices

$$\begin{aligned} & \text{conv}(p'_1, p'_2, \dots, p'_{d+1}, p''_1) \\ & \text{conv}(p'_2, \dots, p'_{d+1}, p''_1, p''_2) \\ & \quad \vdots \\ & \text{conv}(p'_{d+1}, p''_1, p''_2, \dots, p''_{d+1}), \end{aligned} \tag{12}$$

and this way we obtain a simplicial triangulation \mathcal{T}_h of $J \times \Omega$. There holds the following result from [19, Thm. 1].

Theorem 8. *The simplicial partition \mathcal{T}_h is admissible.*

In order to approximate a function in space-time by an element of $\mathcal{S}^1(\mathcal{T}_h)$, we note that $J_h \otimes \Omega_h$ and \mathcal{T}_h have the same set of vertices, and hence $\mathcal{S}^1(J_h; \mathcal{S}^1(\Omega_h))$ and $\mathcal{S}^1(\mathcal{T}_h)$, as well as $\mathcal{S}^1(J_h; \mathcal{S}_0^1(\Omega_h))$ and $\mathcal{S}_0^1(\mathcal{T}_h)$, have the same degrees of freedom. We can therefore define operators

$$\begin{aligned} \mathcal{J}_h &: L^2(H^1(\Omega)) \cap H^1(H_0^{-1}(\Omega)) \rightarrow \mathcal{S}^1(\mathcal{T}_h), \\ \mathcal{J}_{0,h} &: L^2(H_0^1(\Omega)) \cap H^1(H^{-1}(\Omega)) \rightarrow \mathcal{S}_0^1(\mathcal{T}_h) \end{aligned}$$

by requiring $\mathcal{J}_h u$ to have the same values as $\mathcal{J}_h^\otimes u$ at all vertices, likewise for $\mathcal{J}_{0,h}$. We will analyze these new operators by comparing them to their tensor product versions. To that end, the following Lemma will be useful.

Lemma 9. *There holds*

$$\begin{aligned} \|\nabla(\mathcal{J}_h^\otimes u)'\|_{L^2(L^2(\Omega))} &\lesssim \|u\|_{H^1(H^1(\Omega))} + \|u\|_{L^\infty(H^2(\Omega))}, \\ \|\nabla(\mathcal{J}_{0,h}^\otimes u)'\|_{L^2(L^2(\Omega))} &\lesssim \|u\|_{H^1(H_0^1(\Omega))} + \|u\|_{L^\infty(H^2(\Omega))}. \end{aligned}$$

Proof. We will show the second estimate, the first one follows analogously. Note that for $t \in (t_j, t_{j+1})$ we have due to (11)

$$\begin{aligned} \|\nabla(\mathcal{J}_{0,h}^\otimes u)'(t)\|_{L^2(\Omega)} &\lesssim \frac{1}{h} \|u(t_{j+1}) - u(t_j)\|_{H_0^1(\Omega)} + \frac{1}{h} \sum_{k=0,1} \|\Pi_{0,h}(u(t_{j+k})) - u(t_{j+k})\|_{H_0^1(\Omega)} \\ &\lesssim h^{-1/2} \|u'\|_{L^2(t_j, t_{j+1}; H_0^1(\Omega))} + \sum_{k=0,1} \|u(t_{j+k})\|_{H^2(\Omega)}. \end{aligned}$$

An integration in t shows the result. □

Lemma 10. *Let $K \in \mathcal{T}_h$. Then,*

$$\begin{aligned} \|\nabla(\mathcal{J}_{0,h}^\otimes - \mathcal{J}_{0,h})u\|_{L^2(K)} + \|(\mathcal{J}_{0,h}^\otimes u - \mathcal{J}_{0,h}u)'\|_{L^2(K)} &\lesssim h^{-1}\|(\mathcal{J}_{0,h}^\otimes - \mathcal{J}_{0,h})u\|_{L^2(K)} \\ &\lesssim h\|\nabla(\mathcal{J}_{0,h}^\otimes u)'\|_{L^2(K)} \end{aligned}$$

and

$$\|\nabla(\mathcal{J}_h^\otimes - \mathcal{J}_h)u\|_{L^2(K)} + \|(\mathcal{J}_h^\otimes u - \mathcal{J}_h u)'\|_{L^2(K)} \lesssim h^{-1}\|(\mathcal{J}_h^\otimes - \mathcal{J}_h)u\|_{L^2(K)} \lesssim h\|\nabla(\mathcal{J}_h^\otimes u)'\|_{L^2(K)}.$$

Proof. We will only show the estimates involving $\mathcal{J}_{0,h}$, as the ones involving \mathcal{J}_h follow the same lines. The first estimate follows from a standard inverse inequality on polynomial spaces. To see the second, we write $K = \text{conv}\{z_1, \dots, z_{d+2}\}$ and

$$\mathcal{J}_{0,h}^\otimes u|_K = \sum_{j=1}^{d+2} \alpha_j \eta_j + \sum_{j=1}^d \beta_j \nu_j \in \text{span}\{1, t, x_j, x_j t : j = 1, \dots, d\},$$

where $\eta_1, \dots, \eta_{d+2}$ are the hat functions associated to the vertices z_j of K . Here, $1, t, x_j, x_j t$ stand for the functions $(t, x) \mapsto 1$, $(t, x) \mapsto t$, $(t, x) \mapsto x_j$, $(t, x) \mapsto x_j t$. Moreover, we choose ν_j such that these functions vanish in the vertices of K , $\|\nu_j\|_{L^\infty(K)} \lesssim 1$, and $\nabla \nu_j' \simeq h^{-2}$. By definition $\mathcal{J}_{0,h}u$ is affine on K and takes the same values as $\mathcal{J}_{0,h}^\otimes u$ in the vertices of K . Therefore

$$(\mathcal{J}_{0,h}^\otimes - \mathcal{J}_{0,h})u|_K = \sum_{j=1}^d \beta_j \nu_j.$$

Then, scaling arguments, norm equivalence and $\nabla(\nu_j)' \simeq h^{-2}$ show that

$$\|(\mathcal{J}_{0,h}^\otimes - \mathcal{J}_{0,h})u\|_{L^2(K)} \lesssim |K|^{1/2} \sum_{j=1}^d |\beta_j| = h^2 \frac{|K|^{1/2}}{h^2} \sum_{j=1}^d |\beta_j| \simeq h^2 \|\nabla(\mathcal{J}_{0,h}^\otimes u)'\|_{L^2(K)},$$

which finishes the proof. □

Theorem 11. *There holds*

$$\begin{aligned} \|u - \mathcal{J}_{0,h}u\|_{L^2(H_0^1(\Omega))} &\lesssim h(\|u\|_{H^1(H_0^1(\Omega))} + \|u\|_{L^\infty(H^2(\Omega))}) \\ \|(u - \mathcal{J}_{0,h}u)'\|_{L^2(H^{-1}(\Omega))} &\lesssim h(\|u\|_{H^1(H_0^1(\Omega))} + \|u\|_{H^2(H^{-1}(\Omega))} + \|u\|_{L^\infty(H^2(\Omega))}), \\ \|(u - \mathcal{J}_{0,h}u)'\|_{L^2(L^2(\Omega))} &\lesssim h(\|u\|_{H^1(H_0^1(\Omega))} + \|u\|_{H^2(L^2(\Omega))} + \|u\|_{L^\infty(H^2(\Omega))}). \end{aligned}$$

Proof. To show the first estimate, in view of Theorem 7 it suffices to consider $\|\mathcal{J}_{0,h}^\otimes u - \mathcal{J}_{0,h}u\|_{L^2(H_0^1(\Omega))}$. Note that by Lemma 10 we have that

$$\|\nabla(\mathcal{J}_{0,h}^\otimes u - \mathcal{J}_{0,h}u)\|_{L^2(K)} \lesssim h\|\nabla(\mathcal{J}_{0,h}^\otimes u)'\|_{L^2(K)}$$

Summing over all elements $K \in \mathcal{T}_h$ and applying Lemma 9 shows the first of the stipulated estimates. To show the second and third estimate, we will again apply Theorem 7. In order to treat the remaining terms, note that

$$\|(\mathcal{J}_{0,h}^\otimes u - \mathcal{J}_{0,h}u)'\|_{L^2(H^{-1}(\Omega))} \leq \|(\mathcal{J}_{0,h}^\otimes u - \mathcal{J}_{0,h}u)'\|_{L^2(L^2(\Omega))} \lesssim h\|\nabla(\mathcal{J}_{0,h}u)'\|_{L^2(L^2(\Omega))},$$

where the last estimate follows from Lemma 10. Then, we apply Lemma 9 to finish the proof. \square

Theorem 12. *There holds*

$$\|u - \mathcal{J}_h u\|_{L^2(H^1(\Omega))} \lesssim h(\|u\|_{H^1(H^1(\Omega))} + \|u\|_{L^\infty(H^2(\Omega))}).$$

Proof. We note that

$$\|(\mathcal{J}_h^\otimes - \mathcal{J}_h)u\|_{L^2(K)} + \|\nabla(\mathcal{J}_h^\otimes - \mathcal{J}_h)u\|_{L^2(K)} \lesssim h\|\nabla(\mathcal{J}_h^\otimes u)'\|_{L^2(K)}$$

by Lemma 10. The remainder of the proof follows as for Theorem 11. \square

4.1.3 Approximating the heat equation in the energy norm

We have the following result.

Theorem 13. *Let Ω be a convex polygonal domain. Let $u_0 \in H_0^1(\Omega) \cap H^2(\Omega)$ and $f \in H^1(L^2(\Omega))$, and u the solution of the heat equation (1). Suppose that \mathcal{T}_h is a simplicial mesh constructed from a tensor product $J_h \otimes \Omega_h$. Then*

$$\|u - \mathcal{J}_{0,h}u\|_{L^2(H_0^1(\Omega)) \cap H^1(H^{-1}(\Omega))} = \mathcal{O}(h).$$

Proof. It is well known that under the given assumptions, there holds the parabolic regularity $u \in L^\infty(H^2(\Omega))$, $u' \in L^\infty(L^2(\Omega)) \cap L^2(H_0^1(\Omega))$, and $u'' \in L^2(H^{-1}(\Omega))$. According to Theorem 11, we conclude the statement. \square

4.1.4 Approximating the heat equation in the least squares norm

Theorem 14. *Suppose that \mathcal{T}_h is a simplicial mesh constructed from a tensor product $J_h \otimes \Omega_h$. If $u \in L^2(H_0^1(\Omega)) \cap H^1(H^2(\Omega)) \cap H^2(L^2(\Omega)) \cap L^\infty(H^3(\Omega))$, then*

$$\|(u - \mathcal{J}_{0,h}u, \nabla u - \mathcal{J}_h \nabla u)\|_U = \mathcal{O}(h).$$

Proof. The definition of the U -norm and Theorems 11 and 12 show

$$\begin{aligned} \|(u - \mathcal{J}_{0,h}u, \nabla u - \mathcal{J}_h \nabla u)\|_U &\leq \|u - \mathcal{J}_{0,h}u\|_{L^2(H_0^1(\Omega)) \cap H^1(H^{-1}(\Omega))} + \|\nabla u - \mathcal{J}_h \nabla u\|_{L^2(L^2(\Omega))} \\ &\quad + \|(u - \mathcal{J}_{0,h}u)'\|_{L^2(L^2(\Omega))} + \|\operatorname{div}(\nabla u - \mathcal{J}_h \nabla u)\|_{L^2(L^2(\Omega))} \\ &\lesssim h(\|u\|_{H^1(H^2(\Omega))} + \|u\|_{H^2(L^2(\Omega))} + \|u\|_{L^\infty(H^3(\Omega))}). \end{aligned}$$

\square

With respect to the regularity requirements of the last theorem, we state the following.

Proposition 15. *Let $\Omega \subset \mathbb{R}^d$ with $\partial\Omega$ smooth, or, particularly, $\Omega \subset \mathbb{R}$ an interval. Then, if $u_0 \in H_0^1(\Omega) \cap H^3(\Omega)$ and $f \in L^2(H^2(\Omega)) \cap H^1(L^2(\Omega))$ and $f(0) + \Delta u_0 \in H_0^1(\Omega)$, it follows that the solution u of the heat equation (1) fulfills $u \in L^2(H_0^1(\Omega)) \cap H^1(H^2(\Omega)) \cap H^2(L^2(\Omega)) \cap L^\infty(H^3(\Omega))$.*

Proof. It is well known that under the given assumptions, there holds the parabolic regularity $u^{(k)} \in L^2(H^{4-2k}(\Omega))$, $k = 0, 1, 2$. It remains to show that $u \in L^\infty(H^3(\Omega))$. To that end, consider spatial partial derivatives D^α up to third order $|\alpha| \leq 3$. It is clear that $D^\alpha : H^4(\Omega) \rightarrow H^1(\Omega)$ as well as $D^\alpha : H^2(\Omega) \rightarrow \tilde{H}^{-1}(\Omega)$ are bounded and linear operators. Hence, due to Lemma 2, $D^\alpha u \in L^2(H^1(\Omega)) \cap H^1(\tilde{H}^{-1}(\Omega))$, and hence also $D^\alpha u \in C(\bar{J}; L^2(\Omega))$ due to Lemma 1. We conclude that $u \in C(\bar{J}; H^3(\Omega))$. \square

5 Numerical results

In this section we investigate several examples for $d = 1$ (Section 5.1) and $d = 2$ (Section 5.2). For all examples we use $J = (0, 1)$. We define the estimator

$$j(u_h, \sigma_h) =: \eta^2 = \sum_{K \in \mathcal{T}_h} \eta(K)^2$$

where the local error indicators are given by

$$\eta(K)^2 := \|\sigma_h - \nabla u_h\|_{L^2(K)}^2 + \|\partial_t u_h - \operatorname{div} \sigma_h - f\|_K^2 + \|u_h(0) - u_0\|_{\partial K \cap \{0\} \times \Omega}^2.$$

Our adaptive algorithm uses the Dörfler criterion to mark elements for refinement, i.e., find a (minimal) set of elements $\mathcal{M} \subset \mathcal{T}_h$ such that

$$\theta \eta^2 \leq \sum_{K \in \mathcal{M}} \eta(K)^2.$$

Throughout we use the parameter $\theta = 1/4$ in the case of adaptive refinements. If an element K is marked for refinement, i.e., $K \in \mathcal{M}$, it will be (iteratively) subdivided into 2^{d+1} son elements using newest vertex bisection (NVB). In particular, uniform refinement means that each element is divided into 2^{d+1} son elements.

In the figures we visualize convergence rates with triangles where the (negative) slope is indicated by a number besides the triangle. We plot different estimator and respective error quantities over the number of degrees of freedom N . For uniform refinement we have that $h \simeq N^{-1/(d+1)}$.

5.1 Examples in 1+1 dimensions

Throughout this section we consider problems where $\Omega = (0, 1)$. The initial mesh of the space-time cylinder $J \times \Omega$ consists of four triangles with equal area.

5.1.1 Example 1

For the first example we consider the smooth manufactured solution

$$u(t, x) = \cos(\pi t) \sin(\pi x).$$

The data f and u_0 are computed thereof. Since the solution is smooth we expect that the overall error converges at a rate $\mathcal{O}(h)$ which can be observed in Figure 1. We also see that the overall estimator converges at the same rate. Moreover, we observe that the error between u and the approximation u_h at times $t = 0, 1$ in the $L^2(\Omega)$ norm and the error between u and u_h in the $L^2(J \times \Omega)$ norm converge at the higher rate $\mathcal{O}(h^2)$.

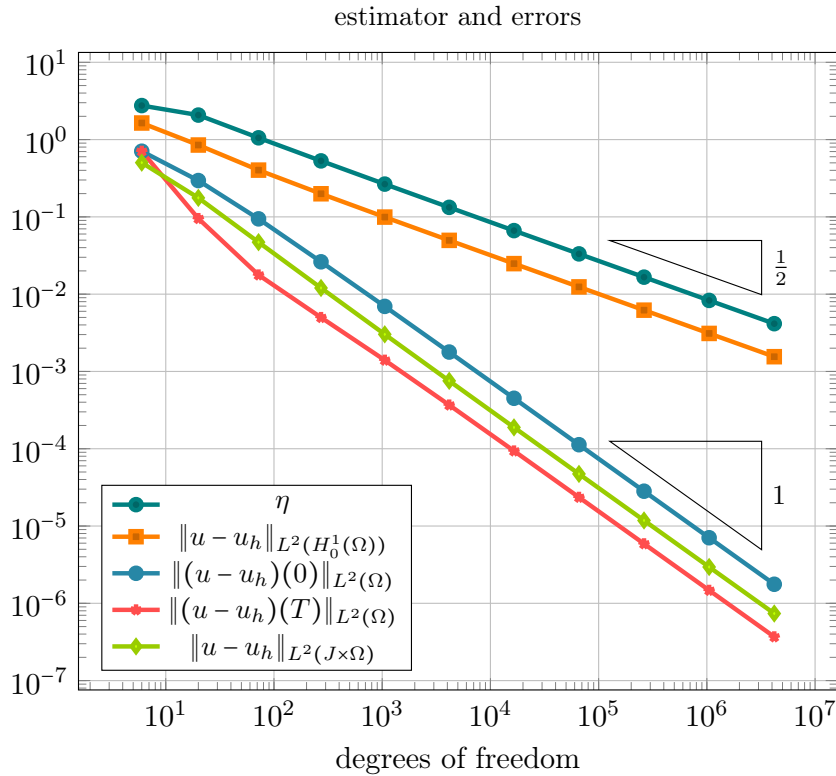


Figure 1: Estimator and errors for the problem from Section 5.1.1.

5.1.2 Example 2

In this case we choose a constant source $f(t, x) = 1$ and as initial data the “hat-function”

$$u_0(x) = 1 - 2 \left| x - \frac{1}{2} \right| \quad x \in \Omega = (0, 1).$$

estimators and errors

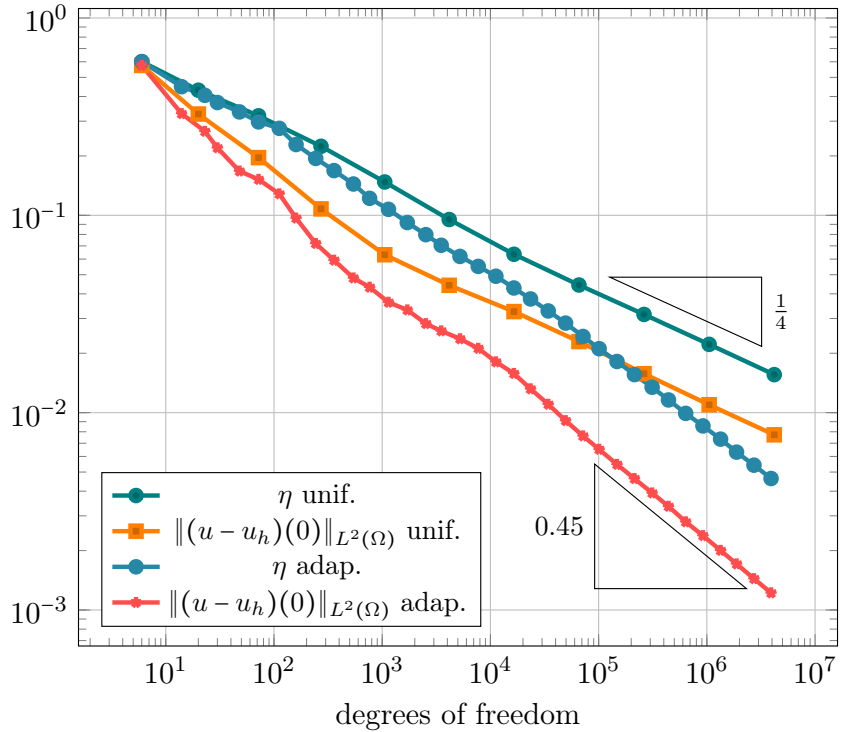


Figure 2: Estimator and errors for the problem from Section 5.1.2.

The overall estimator and the error in the initial data is presented in Figure 2. It can be observed that uniform refinement leads to a rate of $1/4$ with respect to the overall degrees of freedom both for the estimator and the error in the initial data whereas in the case of adaptive refinements we obtain a much better rate of approximately 0.45 .

5.1.3 Example 3

In this example we consider a problem with homogeneous initial data and

$$f(t, x) = \begin{cases} 1 & (t, x) \in \{(s, y) \in (1/10, 1/2) \times (0, 1) : y - 1/20 \leq s \leq y - 1/10\} \\ 0 & \text{else} \end{cases}.$$

This function corresponds to a source that is turned on at time $t = 0.1$ and turned off at $t = 0.5$ and moves with a constant speed to the right. The exact solution is not known and in Figure 3 we compare the overall estimator and the error in the initial time in the cases of uniform and adaptive mesh-refinement. We observe that in the uniform case we obtain a reduced rate of $1/4$

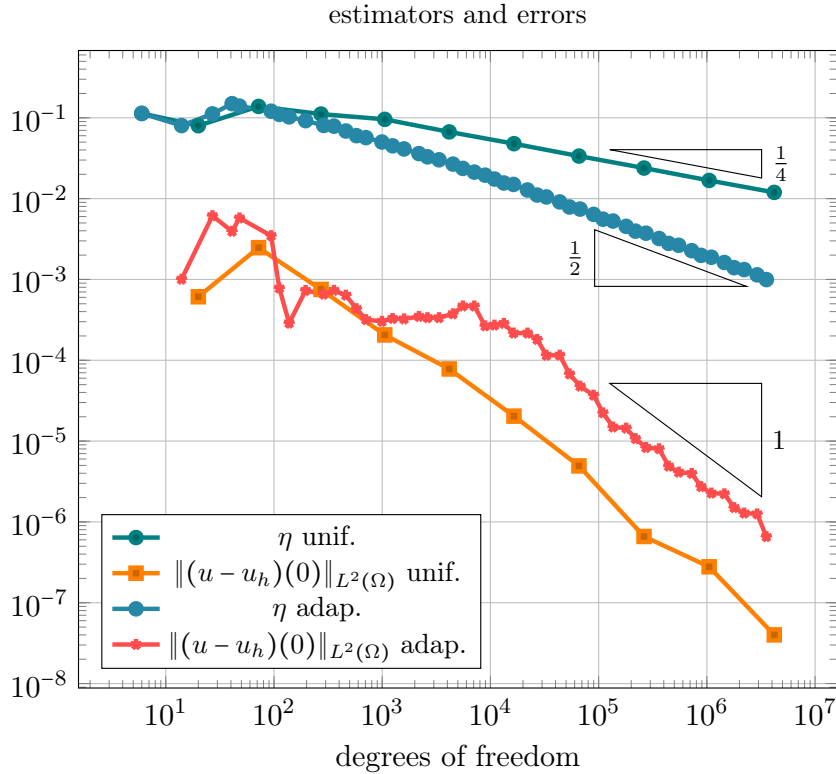


Figure 3: Estimator and errors for the problem from Section 5.1.3.

whereas in the adaptive case a rate of $1/2$ is recovered for the overall estimator. In both cases the error in the initial data converges at the optimal rate.

Figure 4 shows two examples of meshes generated by the adaptive algorithm. Stronger refinements around the support of f can be observed.

5.1.4 Example 4

In this example we set $f(t, x) = 2$, $u_0(x) = 1$. Again, the exact solution is not known to us in closed form. Note that u_0 is regular but does not satisfy homogeneous boundary conditions, i.e., $u_0 \in H^1(\Omega) \setminus H_0^1(\Omega)$.

Figure 5 visualizes the overall estimator and the error at the initial time. For uniform refinements we observe a rate of 0.08 and for adaptive refinements the rate is approximately doubled. We observe a similar behavior for initial data with $u_0 \in L^2(\Omega) \setminus H^1(\Omega)$ which is also used in [1, Section 6.3.4]. We note that reduced rates are also observed in [1].

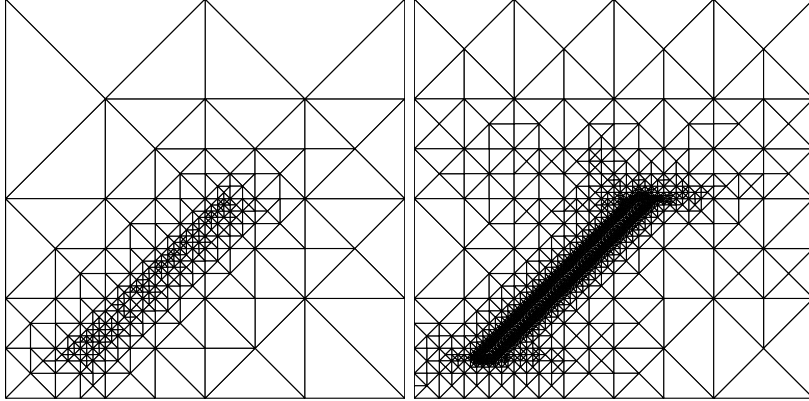


Figure 4: Adaptively generated meshes with 569 (left) resp. 13291 (right) elements for the problem from Section 5.1.3. The vertical axis corresponds to the time coordinate.

5.2 Examples in 2+1 dimensions

5.2.1 Example 1

We consider the domain $\Omega = (0, 1)^2$ and the manufactured solution

$$u(t, x, y) = \cos(\pi t) \sin(\pi x) \sin(\pi y) \quad \text{for } (t, x, y) \in J \times \Omega.$$

The data f and u_0 are computed thereof. We note that the solution is smooth and thus we expect for uniform refinements convergence rates of order h where $h \simeq N^{-1/3}$ and N denotes the overall degrees of freedom. Figure 6 displays the errors and estimator. One observes the optimal behavior for the overall estimator and error as well as higher rates of the initial and end error as well as the error in the L^2 norm of the space-time cylinder. We see a behavior of $N^{-1/2}$ which corresponds to $h^{3/2}$.

5.2.2 Example 2

For this example we consider $\Omega = (-1, 1)^2 \setminus \text{conv}\{(0, 0), (0, -1), (1, -1)\}$ and $u_0(x, y) = 0$. The source f is given by

$$f(t, x, y) = \begin{cases} t & \text{if } \sqrt{x^2 + y^2} < 1/2, \\ 0 & \text{else.} \end{cases}$$

Since Ω has a reentrant corner at the origin we expect that the unknown solution has reduced regularity at this corner. Figure 7 shows the error in the initial time and the overall estimator for both uniform and adaptive refinements. We observe that uniform refinements lead to rates for the overall estimator of approximately 0.2 whereas for adaptive refinements we only see a slightly improved rate of approximately 0.24.

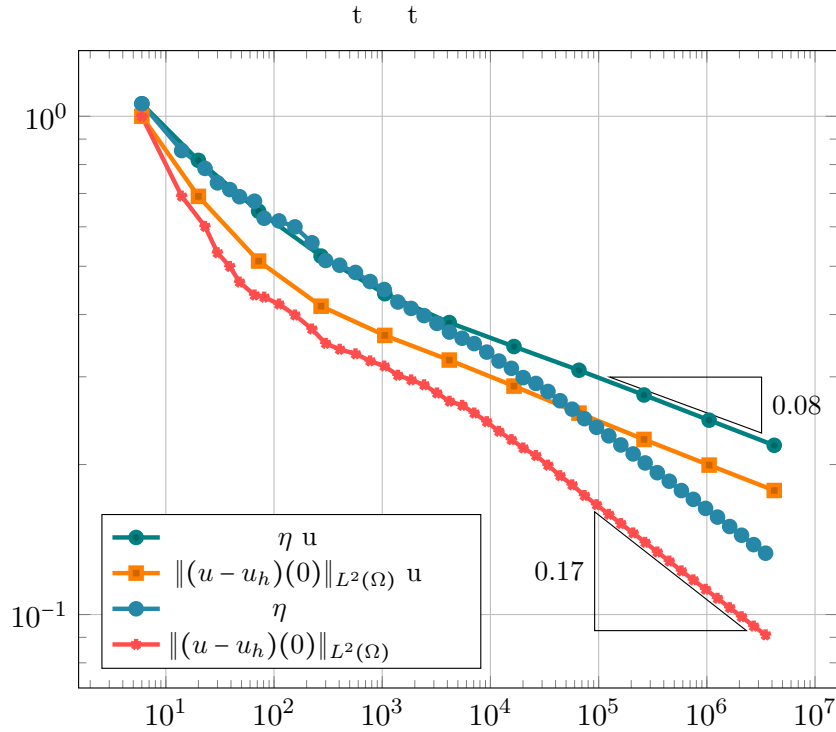


Figure 5: Estimator and errors for the problem from Section 5.1.4.

Figure 8 visualizes the boundary of a space-time mesh obtained by the adaptive algorithm at $t = 0$ (left plot) and $t = 1$ (right plot). One sees that for $t = 0$, where f vanishes, only a few number of elements have been refined. Contrary, when $t = 1$ (right plot), where $f(1, x, y) = 1$ if $x^2 + y^2 < 1/4$, one observes strong refinements close to the boundary of the support of $f(1, \cdot, \cdot)$ but also towards the reentrant corner.

5.2.3 Example 3

For this problem we set $f(t, x, y) = 0$, $u_0(x, y) = 1$ and $\Omega = (0, 1)^2$. Figure 9 shows the error in the initial time and the overall estimator for both uniform and adaptive refinements. We observe a rate of approximately 0.07 for uniform refinement, which is not considerably improved using adaptive refinement.

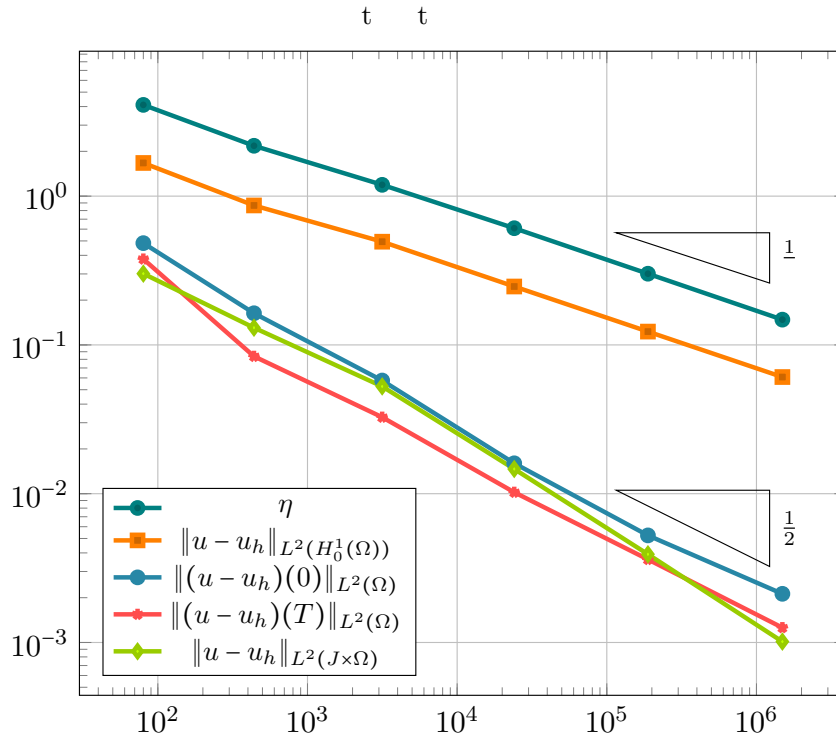


Figure 6: Estimator and errors for the problem from Section 5.2.1.

References

- [1] R. Andreev. Stability of sparse space-time finite element discretizations of linear parabolic evolution equations. *IMA J. Numer. Anal.*, 33(1):242–260, 2013.
- [2] R. Andreev. Space-time discretization of the heat equation. *Numer. Algorithms*, 67(4):713–731, 2014.
- [3] J. Bey. Simplicial grid refinement: on Freudenthal’s algorithm and the optimal number of congruence classes. *Numer. Math.*, 85(1):1–29, 2000.
- [4] P. B. Bochev and M. D. Gunzburger. *Least-squares finite element methods*, volume 166 of *Applied Mathematical Sciences*. Springer, New York, 2009.
- [5] E. Burman and L. Oksanen. Data assimilation for the heat equation using stabilized finite element methods. *Numer. Math.*, 139(3):505–528, 2018.

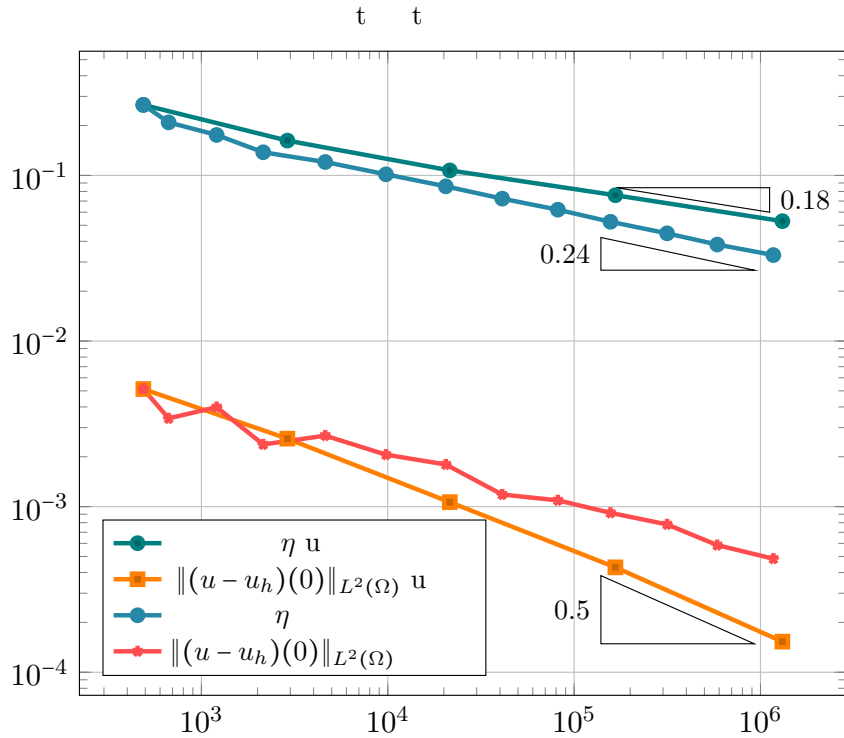


Figure 7: Estimator and errors for the problem from Section 5.2.2.

- [6] R. Dautray and J.-L. Lions. *Mathematical analysis and numerical methods for science and technology. Vol. 5.* Springer-Verlag, Berlin, 1992. Evolution problems. I, With the collaboration of Michel Artola, Michel Cessenat and H el ene Lanchon, Translated from the French by Alan Craig.
- [7] D. Devaud and C. Schwab. Space–time hp-approximation of parabolic equations. *Calcolo*, 55(3):55:35, 2018.
- [8] J. Douglas, Jr. and T. Dupont. Galerkin methods for parabolic equations. *SIAM J. Numer. Anal.*, 7:575–626, 1970.
- [9] E. Fern andez-Cara, A. M unch, and D. A. Souza. On the numerical controllability of the two-dimensional heat, Stokes and Navier-Stokes equations. *J. Sci. Comput.*, 70(2):819–858, 2017.

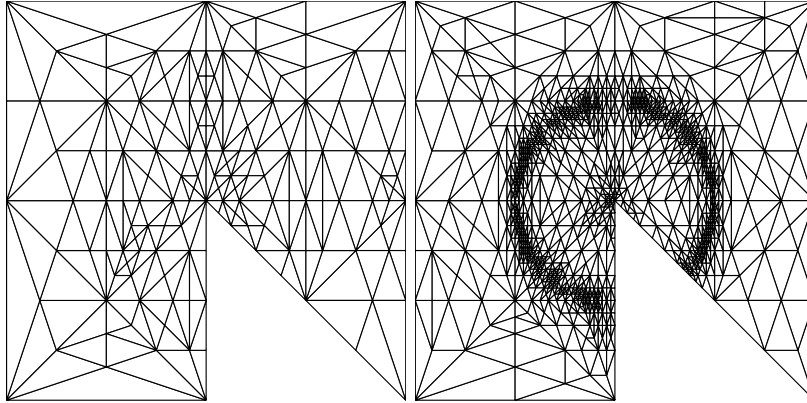


Figure 8: Space-time meshes restricted to $t = 0$ (left) resp. $t = 1$ (right) for the problem from Section 5.2.2. The space-time mesh consists of 149478 elements. The number of boundary elements (triangles) in the left plot is 269 and in the right plot 1932.

- [10] T. Führer and M. Karkulik. New a priori analysis of first-order system least-squares finite element methods for parabolic problems. *Numer. Methods Partial Differential Equations*, 35(5):1777–1800, 2019.
- [11] M. D. Gunzburger and A. Kunoth. Space-time adaptive wavelet methods for optimal control problems constrained by parabolic evolution equations. *SIAM J. Control Optim.*, 49(3):1150–1170, 2011.
- [12] T. Hytönen, J. van Neerven, M. Veraar, and L. Weis. *Analysis in Banach spaces. Vol. I. Martingales and Littlewood-Paley theory*, volume 63 of *Ergebnisse der Mathematik und ihrer Grenzgebiete. 3. Folge. A Series of Modern Surveys in Mathematics [Results in Mathematics and Related Areas. 3rd Series. A Series of Modern Surveys in Mathematics]*. Springer, Cham, 2016.
- [13] D. Kim, E.-J. Park, and B. Seo. Space-time adaptive methods for the mixed formulation of a linear parabolic Problem. *J. Sci. Comput.*, 74(3):1725–1756, 2018.
- [14] U. Langer, S. E. Moore, and M. Neumüller. Space-time isogeometric analysis of parabolic evolution problems. *Comput. Methods Appl. Mech. Engrg.*, 306:342–363, 2016.
- [15] M. Majidi and G. Starke. Least-squares Galerkin methods for parabolic problems. I. Semidiscretization in time. *SIAM J. Numer. Anal.*, 39(4):1302–1323, 2001.
- [16] M. Majidi and G. Starke. Least-squares Galerkin methods for parabolic problems. II. The fully discrete case and adaptive algorithms. *SIAM J. Numer. Anal.*, 39(5):1648–1666, 2001/02.

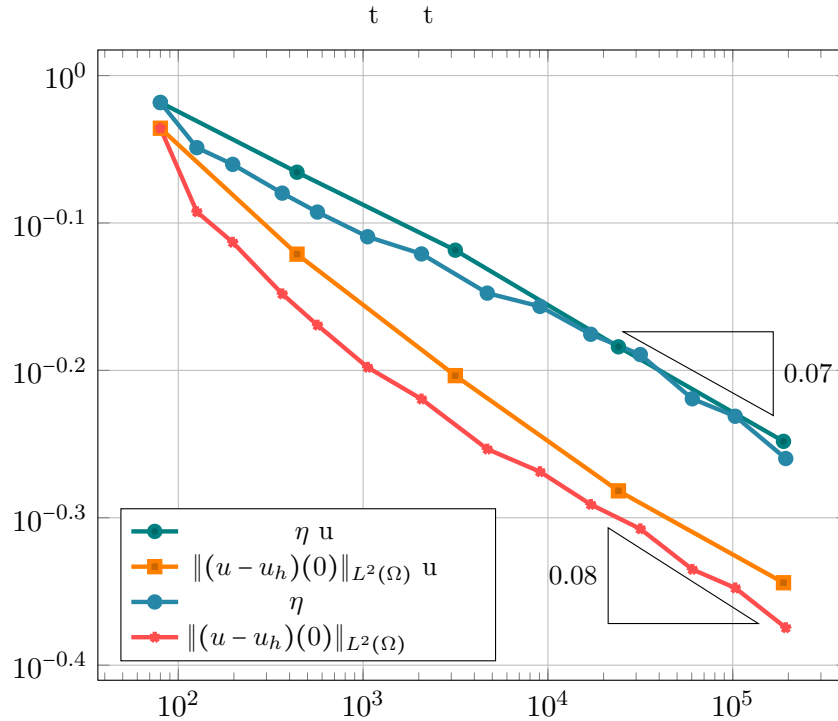


Figure 9: Estimator and errors for the problem from Section 5.2.3.

- [17] M. Montardini, M. Negri, G. Sangalli, and M. Tani. Space-time least-squares isogeometric method and efficient solver for parabolic problems. *Math. Comp.*
- [18] S. E. Moore. A stable space-time finite element method for parabolic evolution problems. *Calcolo*, 55(2):Art. 18, 19, 2018.
- [19] M. Neumüller and E. Karabelas. Generating admissible space-time meshes for moving domains in $d + 1$ -dimensions. Technical report, <https://arxiv.org/abs/1505.03973>, 2015.
- [20] C. Schwab and R. Stevenson. Space-time adaptive wavelet methods for parabolic evolution problems. *Math. Comp.*, 78(267):1293–1318, 2009.
- [21] O. Steinbach. Space-time finite element methods for parabolic problems. *Comput. Methods Appl. Math.*, 15(4):551–566, 2015.
- [22] O. Steinbach and M. Zank. Coercive space-time finite element methods for initial boundary value problems. Technical report, Berichte aus dem Institut für Numerische Mathematik, Bericht 2018/7, TU Graz, 2018, 2018.

- [23] R. Stevenson and J. Westerdiep. Stability of galerkin discretizations of a mixed space-time variational formulation of parabolic evolution equations. Technical report, <https://arxiv.org/abs/1902.06279>, 2019.
- [24] F. Tantardini and A. Veerer. The L^2 -projection and quasi-optimality of Galerkin methods for parabolic equations. *SIAM J. Numer. Anal.*, 54(1):317–340, 2016.
- [25] V. Thomée. *Galerkin finite element methods for parabolic problems*, volume 25 of *Springer Series in Computational Mathematics*. Springer-Verlag, Berlin, second edition, 2006.
- [26] J. Wloka. *Partial differential equations*. Cambridge University Press, Cambridge, 1987. Translated from the German by C. B. Thomas and M. J. Thomas.
- [27] K. Yosida. *Functional analysis*. Classics in Mathematics. Springer-Verlag, Berlin, 1995. Reprint of the sixth (1980) edition.
- [28] E. Zeidler. *Nonlinear functional analysis and its applications. II/A*. Springer-Verlag, New York, 1990. Linear monotone operators, Translated from the German by the author and Leo F. Boron.